Journal of Fundamental and Applied Sciences

ISSN 1112-9867

Available online at http://www.jfas.info

Research Article

FABRICATION AND INVESTIGATION OF STRUCTURAL, OPTICAL AND DIELECTRICAL PROPERTIES OF BISMUTH TRISULFIDE (Bi_2S_3) THIN FILM

H. Benattou*, N. Benramdane, M. Medles

Laboratory for the Elaboration and Characterization of Electronics Materials; Djillali Liabes University; Sidi Bel-Abbes BP 89, 22000, Algeria

Received: 14 April 2017 / Accepted: 29 August 2017 / Published online: 01 September 2017

ABSTRACT

Bismuth trisulfide (Bi_2S_3) in thin films was prepared by spray pyrolysis method at temperature of 280°c. The films were of orthorhombic crystal structure, and direct optical gap of 1.61eV. Tangent of dielectric losses, AC conductivity, dielectric constant and electric modulus were investigated versus the frequency (5Hz-13MHz) and the temperature (293-333°K). The single electric relaxation time is of order of nano-second and DC conductivity from 0.29 to 3.22 $(\Omega.cm)^{-1}$, were indicated from electrical analysis. The observed behavior was described in term of a multi-hopping process. The dependence of 'σ_{AC}' and '*S*' with temperature, were interpreted by the model (*CBH*). The density of the localized states $N(E_f)$ is of order of 10^{20} $cm^{-3}.\Omega^{-1}$, the maximum barrier height W_M of order of 0.1eV, and the activation energy ($E_a \approx 0.12eV$) were calculated for these materials.

Keywords: thin films; Bi_2S_3; spray pyrolysis; AC conductivity; dielectric properties.

Author Correspondence, e-mail: h.benattou@gmail.com

doi: http://dx.doi.org/10.4314/jfas.v9i3.30

1. INTRODUCTION

1.1. Bi_2S_3 Thin films: Properties and Applications

Bismuth trisulfide Bi_2S_3 belongs to the members of the important materials of the V-VI group

of compound semiconductors due to their important properties such us photosensitivity, photoconductivity and thermoelectric power [1, 2, 3, 4, 5]. This material has interesting in the modern technological application such as optoelectronic devices, photo-electrochemical cell, thermoelectric devices [6], photodiode arrays, photoconductors [7,8], IR detectors, and photovoltaic devices [9]. The direct optical gap of this compound is of 1.30eV [10,11], it varied from 1.60 to 1.70eV in form of thin films according to the preparation method. It is located in visible solar energy spectra making it useful for photovoltaic conversion. Based on these last application fields, for integrating the thin films of Bi2S3 into the conversion devices of the solar energy, it is necessary to understand their electrical properties. The direct current conduction studies provide an idea about the conduction of the free charges under the application of an external electric field and alternatif current conduction shows the dependance of conductivity with frequency, where the conduction occurs via the trap levels situated in the gap of the materials. There are many models and reports available on the mechanisms of conduction of different semi conductors materials in thin films, such as the quantum mechanical tunneling (QMT) [12] and the model of the correlated barrier hopping (CBH) [13,14], it have been proposed to explain the mechanism of AC conduction.

Although, these investigations, the electric transport phenomena of the Bi2S3 in thin films are not available, so this investigation is the first.

1.2 Techniques of Deposition of the Bi_2S_3 Thin Films:

We can find several techniques in the literature illustrate the preparation of the thin films of Bi2S3: Chemical bath deposition method [15, 16], SILAR method [17], and spray pyrolysis [3,18]. Among these methods, spray pyrolysis is a truly low-cost technique which we were adapted in this investigation for the fabrication of our thin films from a solution of bismuth chloride and thiourea.

2. RESULTS AND DISCUSSION

2.1 Structural properties

Our thin films obtained were opaque and of color of metallic gray, they were perfectly adhered to the substrate surfaces. The various diffractions peak existing in Fig.1 are narrower

and well intense indicating the crystallisation of the material with orthorhombic crystal structure. Highly satisfactory agreement was seen between the inter-reticular distance of our films and those of the powder standard card N°: 43-1471.

The lattice parameters ‘a, ‘b’ and ‘c’ calculated are respectively of: 11.0696Å, 11.12 Å and 3.968Å**.** The crystallite size evaluated from full width half maximum (FWHM) of the slow scan of XRD peak (310) at 2θ =25.24° is about of 222.76Å. This result confirms also that our films are of nanocrystalline structure (22.276nm). The crystallite size is influenced by the conditions of the preparation of the films.

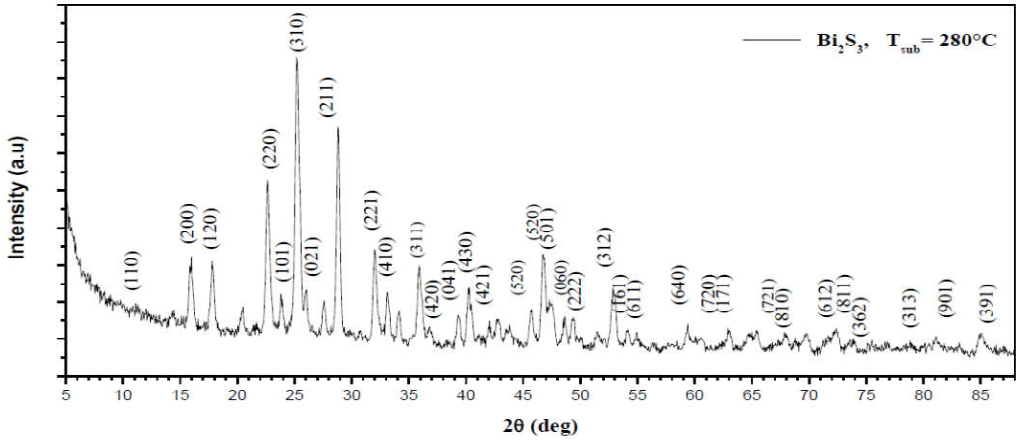

Fig.1. X- ray diffraction diagram of Bi_2S_3 film prepared at substrate temperature of 280°c.

2.2 Optical properties

Fig.2 shows the transmittance (T%) and the reflectance (R%) spectrum of Bi_2S_3 films in the range of 200-2500nm at room temperature. We can distinguish tree regions: the first situated in the visible wavelength range varied between 200-790nm, it is characterized by the very down transmission and the strong absorption (see Fig.3). The second region situated in the wavelengths range varied between 790-1720nm, the optical transmission of Bi_2S_3 film is higher, it presents the transmission threshold around λ=790 nm, the transmission of the film increases to 44%, this is caused by the lack of material in some places, a highly absorption coefficient values in Fig.3 (in order of 10^4 cm^{-1}) are assigned of lacking or condensation nature in the material. Last region is of the decreasing transmission from the wavelength λ=1800nm, the value of the transmission of the film start to decrease which it present a loss in the material transparence. The reflectance spectrum of Bi_2S_3 films shows a sufficiently wide

band in the near red infrared wavelength range situated between 1476-1826nm presenting a minimum around λ=1615nm. The absorption coefficient spectrum provides information about electronic transition nature and the band gap of our material. Bi_2S_3 has a band structure *E(k)* where the maximum of the valence band and the minimum of the conduction band are aligned (direct band gap) [18]. The allowed direct transition is very appropriate in the transition nature of our material; consequently we evaluated the energy of the optical gap (*Eg*) using the curve $(\alpha h\nu)^2$, we extrapolated the linear portion of this curve cross the energy axis at *Eg* (see Fig.4), the value of the direct band gap was found to be 1.61eV.

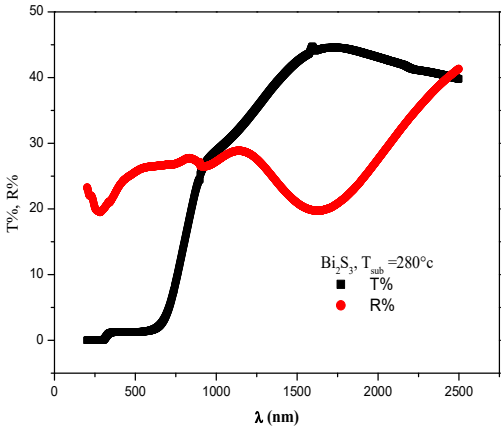

Fig.2. T% and R% spectrum of Bi_2S_3 films

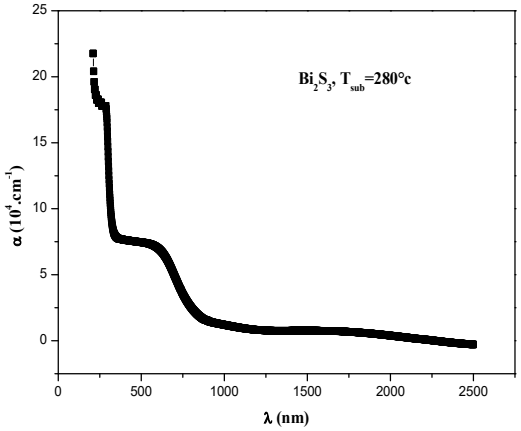

Fig.3. Absorption coefficient (α) of Bi_2S_3 films versus wavelength (λ)

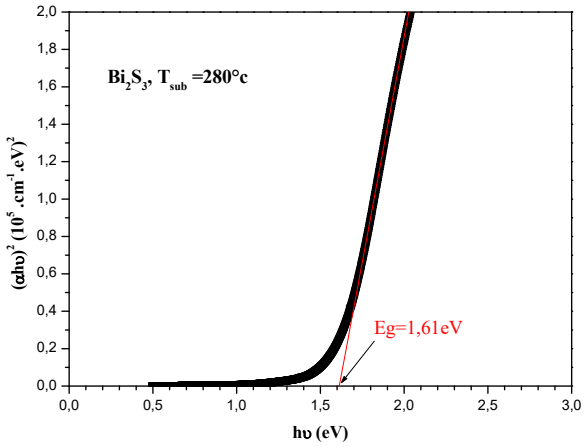

Fig.4. Variation of $(\alpha h\upsilon)^2$ versus $(h\upsilon)$ for the Bi_2S_3 film prepared at T_{sub}=280°C.

2.3. Electric Properties

Complex impedance diagrams (Z" vs. Z') of Bi_2S_3 in thin films are displayed in Fig.5. These

diagrams are for samples which were prepared at T_{sub}=280°C and were heated in the temperature range of 293-333°K. The diagram exhibit one semicircular for each heating temperature selected before. We can see that the semi circles are slightly inclined and their centers are shifted under the real axis. The presence of the semi circular arc was interpreted by the grain contribution. It indicates also a single relaxation process occurring in the film. The resulting semi circlar arc is equivalent to a parallel RC circuit [19, 20], where R and C are resistance and capacitance of the film, respectively; R was given by the diameter of semi-circular arc and C was determined by the relation: $RC\omega_{max} = 1$, which holds a maximum of semicircle, or by the fit of the curves (Z' vs. fr) and (Z" vs. fr). The impedance in complex form associated at this case is expressed as:

$$Z^* = \frac{R}{1 + jRC\omega} = Z' - jZ'' \qquad (2)$$

$$Z' = \frac{R}{1 + (RC\omega)^2} \qquad (3)$$

$$Z'' = \frac{R^2 C\omega}{1 + (RC\omega)^2} \qquad (4)$$

Where, 'ω' is angular frequency. Fig.5 also shows that increase in temperature leads to decrease in size of the semicircle, corresponding to a shift in the center of the semicircle toward origin of the plot of the impedance spectrum. At each selected temperature, the diameter of the semicircle represent the value of the resistance R of the film; it decreases with increases in the temperature, result an increase in conductivity, indicating a semiconducting behavior of this component [21].

In the curve (-Z" vs. fr) of Fig.6, the variation in imaginary part of complex impedance versus frequency and temperature, shows that the values of the Z" reach a maximum indicating a single relaxation process. The maximum of peaks shifts toward high frequencies with the increase in the temperature indicates the increase in dielectric losses. The relaxation time 'τ' was evaluated (see table.1) by the angular relaxation frequency (ω_{max}) at the maximum peak of Z" as given in the following formula:

$$\omega_{max} . \tau = 1 \qquad (5)$$

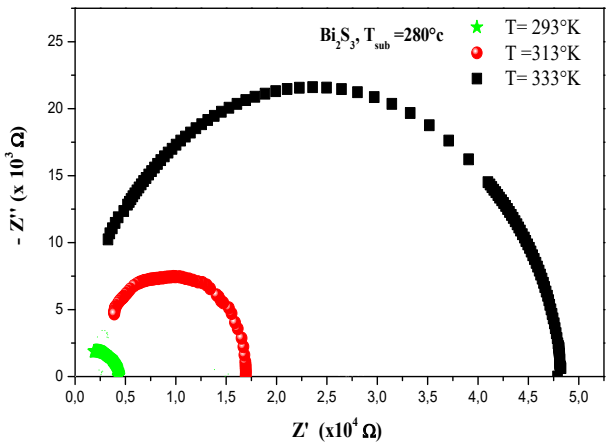

Fig.5. Complex impedance diagrams (-Z" vs. Z') of Bi_2S_3 thin film.

We notice a displacement of the relaxation peak towards the low frequencies with variation in the temperature. This phenomenon display that the frequency of the peak indicate behavior of Arrhenius type. In the curve (Z' vs fr) of Fig.7, the real part of complex impedance decreases with the temperature showing behavior of a semiconductor [21,22].

The tangent of dielectric losses 'tanδ' is expressed as that given in formula (6). It's a parameter of dielectric material; it quantifies the dissipation of electric energy in the material.

$$tan\delta = \frac{Z''}{Z'} = \frac{\varepsilon''}{\varepsilon'} \qquad (6)$$

In Fig.8, we draw 'tanδ' versus frequency and temperature. Relaxation peaks can not be seen in the frequency range used in this study. However, B.Ouni [21] has been verified that in the absence of a well defined tanδ peak, he can obtained 'τ' from the diagram of the complex impedance (Z").

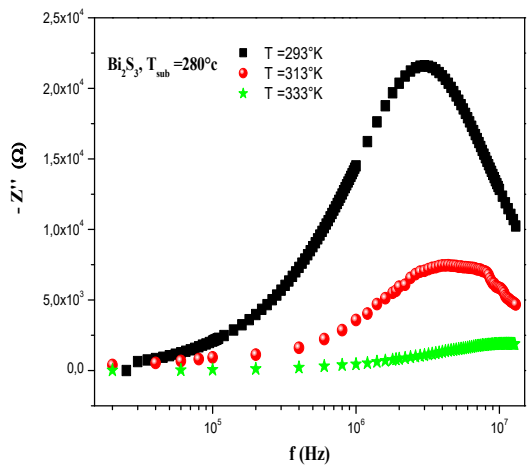

Fig.6. the variation of the Z'' with frequency and temperature for Bi_2S_3 film deposited at T_{sub}=280

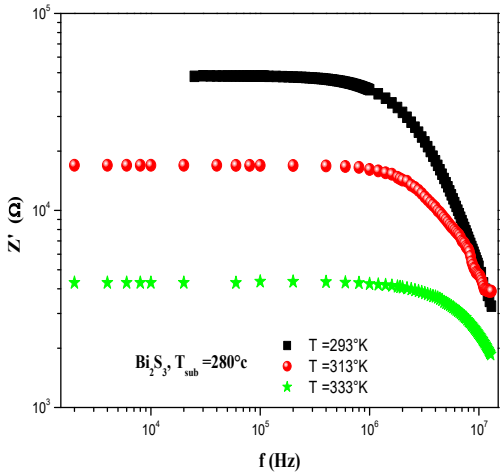

Fig.7. the variation of the Z' with frequency and temperature for Bi_2S_3 film deposited at T_{sub}=280

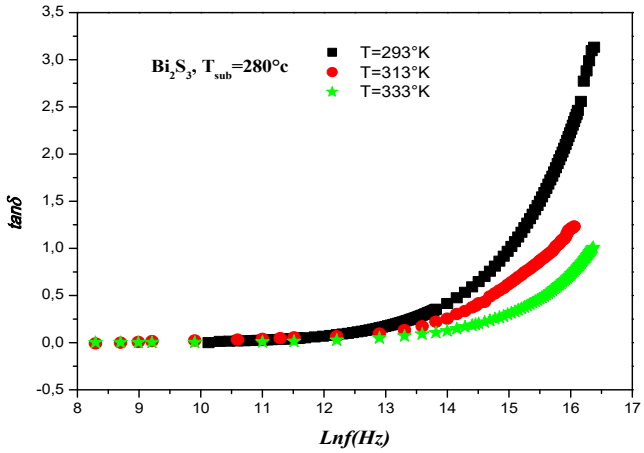

Fig.8. tanδ versus frequency and temperature

2.3.1. Study of AC conductivity as a function of frequency and temperature:

AC conductivity (σ_{AC}) of our thin films was calculated versus frequency and temperature from the complex impedance (Z*), we used the following formula:

$$\sigma^* = \frac{1}{Z^*}\frac{L}{W.d} \qquad (7)$$

Where, 'W' is the length of the electrode; d is the thickness of the sample to be characterized,

and ‘L’ is the distance between the two electrodes. Fig. 9 shows the dependence of conductivity on frequency (5Hz–13MHz), at different selected temperatures (293°K, 313°K and 333°K) on a log–log scale. We observe that conductivity gradually increase with increases in frequency and temperature having different slopes over two frequency regions. The first region, in low frequency, the conductivity is independent of the frequency. In this region, σ_{DC} may be calculated (see table.1). While at higher frequency (second region), AC conductivity (σ_{AC}) follows an approximate behavior of power-law type [23]. This response is characteristic of ionic conductors [24, 25, 26]. The formula for conductivity is written as follows.

$$\sigma_{AC}(\omega) = \sigma_{DC} + A.\omega^{S} \qquad (8)$$

Where ‘A’ is a constant, ‘ω’ is the angular frequency, and ‘S’ is the exponent of the frequency component which normally takes the value less than or equal to unity. This variation is indicative of localized conduction. In the case where the conductivity decreases with the frequency, the conduction model is said: free band conduction [27]. We can see also, that AC conductivity increases with increase in temperature. This rise of the σ_{AC} with temperature is attributed to thermal activation which allows the hopping of carriers between different localized states. Besides, this increases in the conductivity with the temperature, indicates the semiconductor nature of the films. It is due to the good crystallinity of the films, which increases the mobility of the charge carriers. Several authors have reported similar behavior by nanocrystalline materials prepared by different methods [28]. So our crystallites are nanometric also. In the literature there are various models which have been developed to explain the dependence of conductivity at frequency and temperature in materials and it is known that the low values of the frequency exponent 'S' indicate the multi-hop process, While the high values of 'S' indicate the single hop process [27]. For our studied sample, the values of the frequency exponent 'S' obtained from the slopes of the AC conductivity in the high frequency region are listed in Table 1. In our case, the parameter ‘S’ has smaller values, where $0<S<0.5$, indicating multihopping process, it decreases with the temperature in the range of 293-333°K. Various models have been proposed by the investigators to discuss the behavior of ‘S’ of chalcogenide compounds [29]. The correlated barrier hopping (CBH) model is the most widely model used to describe the AC conductivity of amorphous semiconductors. This

model consider the electron pairs hope from doubly occupied D+ stated to a nearly D- center over the barrier separating the two sites. The expression for 'S' obeys the formula:

$$S = 1 - \frac{6k_BT}{W_M + k_BTln(\omega\tau_0)} \qquad (9)$$

Where W_M is the maximum barrier height at infinite intersite separation, τ_0 is the relaxation time which is in order of an atom vibrational period ($\tau_0 \approx 10^{-13}$ sec).The temperature dependence of σ_{AC} is most likely due to the hopping process. We can suggest that the conduction occurs by hopping assisted by phonon between localized states near the Fermi level 'E_F'. Consequently and according to the Austin and Mott theory [30], the AC conductivity is given by the formula (10):

$$\sigma_{ac}(\omega) = \frac{\pi}{3}e^2k_BTN(E_F)^2\alpha^{-5}\omega\left[Ln\left(\frac{\Omega}{\omega}\right)\right]^4 \qquad (10)$$

Where '*e'* is the electronic charge, 'α' describes the decay of the localized state wave function and Ω is the phonon frequency. By assuming Ω =10^{13} Hz and α =0.3 nm^{-1} [31]. $N(E_F)$ is calculated from the plot of$\sigma(\omega)\left[Ln\left(\frac{\Omega}{\omega}\right)\right]^{-4}$ versus the frequency. It's found that it is of order of $10^{20}\, eV^{-1}.cm^{-3}$, which increases as $\sigma_{ac}(\omega)$ with temperature as seen in table.1. The higher value of $N(E_F)$ is related to the increase in the number of load carriers in the band gap under the temperature effect.

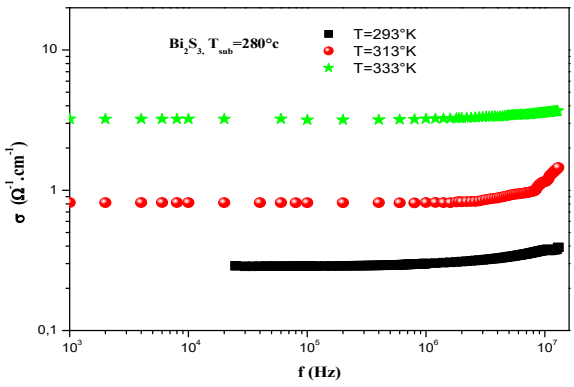

Fig.9. AC conductivity versus frequency and temperature

2.4. Dielectric Properties

2.4.1 Dielectric Constants Study*:* Under the influence of an electric field applied to a

material, the response is corresponding to the load carriers which are electrons in the conductors, or ions in the ionic conductors. In the insulating material, the response corresponds to the polarization which corresponds to the displacement local of electrons, and the orientation of the dipoles. Fig.10 shows the frequency and temperature dependence of the dielectric constant ε' for Bi_2S_3, It is observed that the dielectric constant ε' appears to be depend of temperature and frequency. So, the decrease of ε' as function of frequency at the constant temperature can be attributed to the contribution of multi components of polarizability, like deformational which concerns the electrons or ions, and relaxation concerns the orientation or interfacial [32]. As the applied field frequency is increasing, the orientation polarization tends to decrease since it takes more time than those others polarizations, electronic or ionic polarization, and consequently ε' tends to reduce, approaching a constant value, at high frequencies, due to the space charge polarization. On other hand, the increase of the dielectric constant ε' with temperature can be assigned to the fact that the bound charge carriers get gradually an quantity of thermal excitation energy to be able to respond to the change in the external field more easily, their orientation is facilitate their orientation is facilitate when the temperature increases, the orientational polarization increases also, and in turn increases ε'.

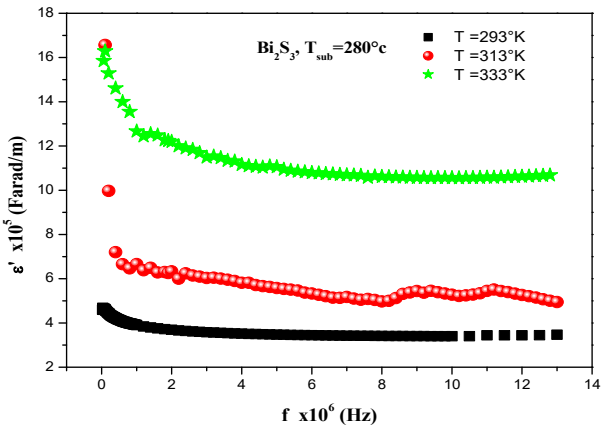

Fig.10. ε' versus frequency and temperature

Fig.11 shows the variation of ε" with frequency and temperature for our sample, we observe that ε" decreases with increasing frequency at constant temperature, and it increases by

increasing temperature at constant frequency. Dielectric constant is composed of two contributions: the first is from the DC conduction at low frequency and the second is from the dielectric polarization processes at high frequency. At low and moderate frequencies, as the temperature increases, the conductivity increases too, bringing to the high value of the dielectric constant, ε"(ω). This is in agreement with equation: $(\varepsilon^{"} = \sigma_{AC}/\varepsilon_0\omega)$. AC conductivity ($\sigma_{AC}$) can be mixed up with DC conductivity (σ_{DC}) like was given in formula (8). ε"(ω) decreases with increasing frequency which results in rapid polarization processes occurring in the Bi_2S_3 films under applied field. Indeed, when the frequency increases, AC conductivity follows a power law $(A.\omega^S)$ and then ε"(ω) can be written as a power law too $(\varepsilon^{"} = A.\frac{\omega^S}{\varepsilon_0\omega} = B.\omega^m \; and \; m = S - 1)$ whose exponent m is negative (see equation 12), this function decreases greatly, it depends on the values of the power. We can indicate these behavior in The shape of ln(ε″) vs ln(f) which shows straight lines with different slopes (Fig. 12). It decreased linearly with temperature according to Giuntini [33]:

$$\varepsilon^{"} = (\varepsilon_0 - \varepsilon_\infty)2\pi^2 N(ne/\varepsilon_0)k_B T\tau_0^m W_m^{-4}\omega^m \quad (11)$$

$$m = -\frac{4k_B T}{W_M} \quad (12)$$

Where, W_M is the maximum barrier height, its value calculated from equation (12), it is equal to 0.1eV. This value is in good agreement with that obtained by the theory of the hop of the charge carriers over a potential barrier such as that suggested by Elliott [34, 35] and Ghosh [14] in the chalcogenide glasses.

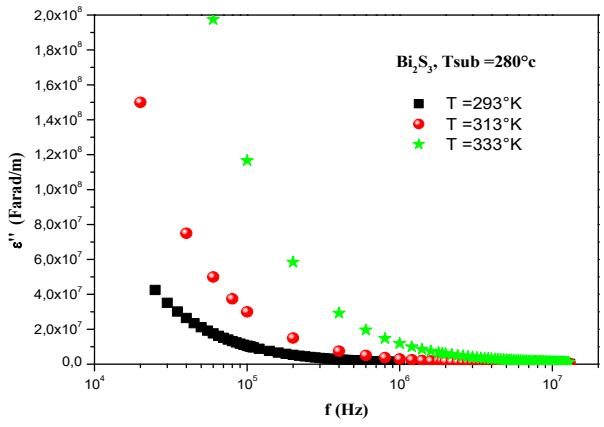

Fig.11. ε'' vs frequency and temperature

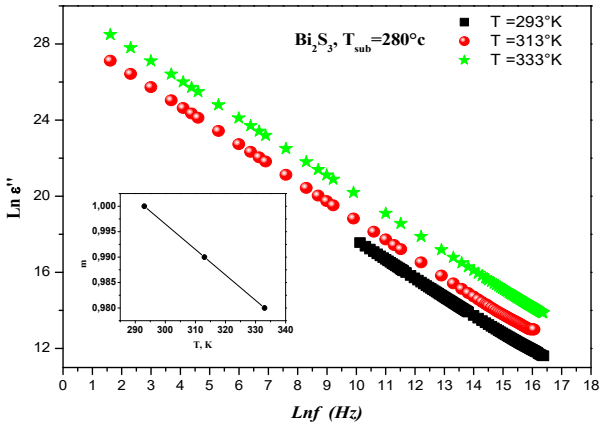

Fig.12. ln ε″ vs. lnf

2.4.2. Electric Modulus Studies: The relaxation mechanisms in the chalcogenide and amorphous materials are represented by several dielectric parameters: dielectric constant, loss tangent, and electric modulus. In the modulus formalism, which we are adopted in this part, the electric modulus ($M^*(f)$) in the complex form (with their two parts: real and imaginary parts) is defined in the term of the complex permittivity ($\varepsilon^*(f)$) as the equation (13):

$$M^*(f) = \frac{1}{\varepsilon^*} = \frac{1}{\varepsilon' - j\varepsilon''} = \frac{\varepsilon'}{\varepsilon'^2 + \varepsilon''^2} + j\frac{\varepsilon''}{\varepsilon'^2 + \varepsilon''^2}$$

$$M^*(f) = M'(f) + jM''(f) \qquad (13)$$

Fig.13 and Fig.14 respectively display the frequency dependences of $M'(f)$ and $M''(f)$ for Bi_2S_3 as a function of temperature. $M'(f)$ shows a dispersion region in the higher frequencies which $M'(f)$ tend to the higher values (Fig.13), while $M''(f)$ exhibits a maximum centered at this region of $M'(f)$. In Fig.14, position of the peak shifts to higher frequencies as the temperature is increased. The frequency region below peak maximum detemines the range in which charge carriers are mobile on long distances. At frequency above peak maximum, the carriers are confined to potential wells, being mobile on short distances, The frequency f_{max} (corresponding to M''_{max}) gives the most probable relaxation time τ_{max} from the condition $\tau_{max}.\omega_{max} = 1$. The relaxation time τ_{max} is proportional to $exp(-E_a/k_B.T)$ with activation energy $E_a \approx 0.12eV$, like it is shown in the inset of Fig.14. and tabeled in Table 1.

Table 1: Parameters of Bi_2S_3 in thin films

	293°K	**313°K**	**333°K**
τ [NanoSec]	53	36.1	14.2
R [KΩ]	47.049	18.638	10.92
C [P.Farad]	1.0933	1.787	1.638
σ_{DC} [$\Omega^{-1}.cm^{-1}$]	0.29	0.82	3.22
S	0.24	0.14	0.12
$N(E_F)$ x10^{20} [$eV^{-1}.cm^{-3}$]	5.11	8.27	15.96
E_a [eV]	0.118	0.124	0.133

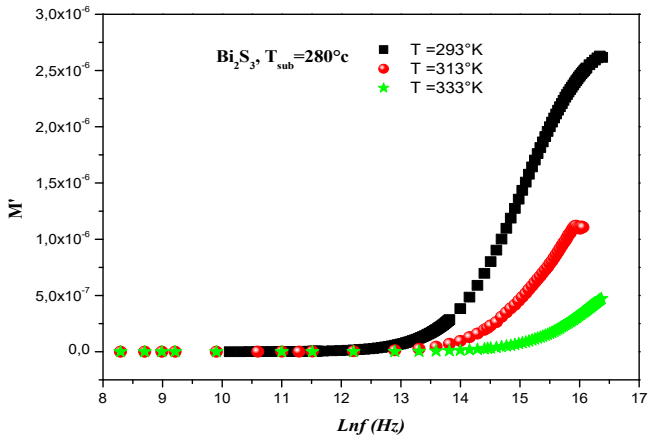

Fig.13. M' (Real part of the electric modulus) vs frequency and temperature

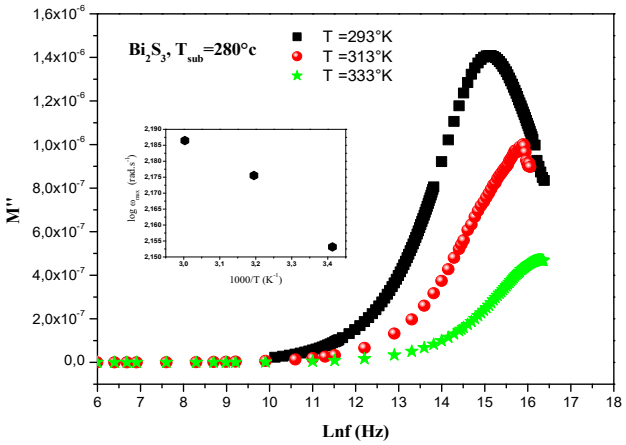

Fig.14. M'' (imaginary part of the electric modulus) vs frequency and temperature.

3. EXPERIMENTAL

The films were prepared by taking equimolar solutions of bismuth chloride and thiourea in appropriate volumes to obtain a Bi:S ratio of 2:3. The mixed solution was sprayed onto a hot glass substrate at the temperature of 280°C. X-ray diffraction (XRD) analysis was carried out

by a Bruker's X-ray Diffractomter (D8 Advance type) with CuKα radiation (λ = 0.15406 nm) over the 2θ collection of data from 5° to 88°. UV–vis–NIR spectra of the transmittance and reflectance were recorded at normal incidence. The range of the wavelengths of 200–2500nm operated, was offer by UV-Visible JASCO type V-570 double beam spectrophotometer. For the AC measurement, our samples were made in the coplanar configuration; the threads of Ohmic electrodes of copper were formed by sticking it on the film using the conducting silver. The dielectric and AC conduction measurements were performed on the Bi_2S_3 sample using an HP4192 impedance meter operating in the range of frequencies of 5Hz- 13MHz for different temperatures (293-333°K). Digital thermocouple was used for temperature controls.

4. CONCLUSION

Bi2S3 thin films have been successfully deposited by the spray pyrolysis technique at substrate temperature of 280°c. X-ray diffraction study of Bi_2S_3 thin film was confirmed orthorhombic Bi_2S_3 crystal structure. The analysis of optical data showed that the thin film of Bi_2S_3 is a semiconductor with the allowed direct transition and a direct band gap value of 1.61eV. Consequently, the Bi2S3 is useful for fabrication of optoelectronic devices. Furthermore, the experimental results obtained in this work in the parts of electric and dielectric studies demonstrated good response to the applied electric field, indicating the fact that the film can be employed in photovoltaic conversion devices.

6. REFERENCES

[1] Ghosh C, and Verma B P. Optical properties of amorphous and crystalline Sb_2S_3 thin film. Thin Solid Films., 1979, 60:61-65

[2] Ghosh C, and Verma B P. Some optical properties of amorphous and crystalline antimony trisulphide thin films. Solid State Commun., 1979, 31:683-686

[3] Kebbab Z, Benramdane N, Medles M, Bouzidi A, and Tabet-Derraz H. Optical and photoelectrical properties of Bi_2S_3 thin films obtained by spray pyrolysis technique. Solar Energy Materials & Solar Cells., 2002, 71: 449–457

[4] Panmand R P, Kawade U V, Kulkarni M V, Apte S K, Kale B B, and Gosavi S W. Synthesis and characterization of Bi_2S_3 nanocrystals in glass matrix. Mater Sci Eng B., 2010: 168-161

[5] Dipalee J D, Shaikh S, Siddiqui F, Ravikiran B, Ravikiran L, Ghule A, and Ramphal Sh. Enhancement of photosensitivity by annealing in Bi_2S_3 thin films grown using SILAR method. Composites: Part B., 2013, 46:1–6

[6] Xie W, Tang X, Yan Y, Zhang Q, and Tritt T M. High thermoelectric performance BiSbTe alloy with unique low-dimensional structure. J. Appl. Phys., 2009, 105

[7] Mane R S, Sankapal B R, and Lokhande C D. Photoelectrochemical (PEC) charadterization of chemically deposited Bi_2S_3 thin films from non aqueous medium. Mater. Chem. Phys., 1999, 60:158–162

[8] Konstantatos G, Levina L, Tang J, and Sargent E H. Nano. Lett., 2008, 8:4002–4006

[9] Yanqiao L, Yange Z, Yan L, Pinjiang L, Huimin J, Hongwei H, and Zhi Z. In situ fabrication of Bi_2S_3 nanocrystal film for photovoltaic devices. Materials Science and Engineering B., 2012, 177:1764– 1768

[10] Black J, Conwell E M, Seigle L, and Spencer C W. Electrical and optical properties of some $M_2^{V\text{-}B}N_3^{VI\text{-}B}$ semiconductors. J Phys Chem Solids, Pergamon Press., 1957, 2:240-251

[11] Nomura R, Toyasaki T, and Matsuda H. Continuous changes of optical band gap energy in thin films of BixSb2-XS3 solid solutions (x= 0 to 2) prepared by solution pyrolysis of dithiocarbonate complexes. Thin Solid Films., 1991, 195:L1-L4

[12] Gubanov A.I. Quantum electron theory of amorphous conductors. New-York (Eds.), 1965.

[13] Elliot S R, AC conduction in amorphous chalcogenide and PNICTIDE semiconductors. Adv. Phys., 1987, 36:135-218

[14] Ghosh A., Phys. Rev. B. 1990, 41, 1479, doi: 10.1103/PhysRevB.41.1479

[15] Chao G, Honglie S, and Lei S, Preparation of nanowall Bi_2S_3 films by chemical bath deposition. Applied Surface Science., 2011, 258: 89– 92

[16] Chao G, Honglie S, Zhou S, and Lei S, Influence of SnS buffer layers on the growth and properties of nanostructured Bi_2S_3 films by chemical bath deposition, Applied Surface Science., 2011, 257: 4439–4442

[17] Ubale A U, Daryapurkar A S, Mankar R B, Raut R R, Sangawar V S, and Bhosale C H, Electrical and optical properties of Bi2S3 thin films deposited by successive ionic layer adsorption and reaction (SILAR) method, Mater. Chem. Phys., 2008, 110:180-185

[18] Benramdane N, Latreche M, Tabet H, Boukhalfa M, Kebbab Z, and Bouzidi A, Structural and optical properties of spray-pyrolysed Bi_2S_3 thin films, Materials Science and Engineering B., 1999, 64: 84–87

[19] Gerhardt R.A. Impedance spectroscopy and mobility spectra. Encyclopedia of Condensed Matter Physics, Georgia Institute of Technology. Atlanta, GA, USA, 2005, pp. 350–363.

[20] Ross Macdonald J. Fundamentals of impedance spectroscopy: emphasizing solid materials and systems. John Wiley & Sons (Eds.), New York: Academic Press, 1987.

[21] Ouni B, Haj Lakhdar M, Boughalmi R, Larbi T, Boukhachem A, madani A, Boubaker K, and Amlouk M, Investigation of electrical and dielectrical properties of Sb_2O_4 semiconductor thin films for TCO and optoelectronic applications, J. Non-Crystalline Solids., 2013, 367: 1-7

[22] Badapanda T, Senthil V, Rout S K, Cavalcante L S, Simões A Z, Sinha T P, Panigrahi S, deJesus M M, Longo E, and Varela J A, Refinement, microstructure, conductivity and impedance properties of Ba[Zr0.25Ti0.75]O3 ceramic, Curr. Appl. Phys., 2011, 11(6):1282–1293

[23] Jonscher AK, Frequency dependence of conductivity in hopping systems, Journal of Non-Crystalline Solids., 1972, 8(10):293-315

[24] Mott N. F, and Davis E. A. Electronic processes in non-crystalline materials, 2nd Eds., Clarendon: Oxford, 1979.

[25] Yoshiyagawa M, and Tomozawa M, Electrical properties of rapidly quenched lithium-silicate glasses, Colloque C9, suppl. 12, Tome 43, Paris: J. Phys, 1982, C9-411

[26] Niklasson G A, Comparison of dielectric response functions for conducting materials, J. Appl. Phys., 1989, 66: 4350-4359

[27] Tewari S, Bhattacharjee A, and Sahay P P, Studies on A.C. conductivity of spray deposited ZnO thin films, Journal of Science and Technology: Physical Sciences and Technology., 2010, 5(II):216-219

[28] Mane R S, Sankapal B R, and Lokhande C D, Studies on chemically deposited nanocrystalline Bi_2S_3 thin films, Materials Research Bulletin., 2000, 35:587–601

[29] Nagels PR. Structure and Bonding in Non-Crystalline Solids, GE. Walrafen and A. G. Revesz (Eds.), New York: Plenum, 1983.

[30] Austin I G, Mott N F. Adv. Phys., 1969, 41-102, doi: 10.1080/00018736900101267

[31] Khelfa A, Benramdane N, Guesdon J P, and Julien C, AC conductivity of amorphous indium-selenium films, Semicond Sci Technol., 1994, 9:1-4

[32] Chi Kao K. Dielectric Phenomena In Solids: With Emphasis On Physical Concepts of Electronic Processes. San Diego, California, USA: Elsevier Academic Press, 1900.

[33] Giuntini J C, and Zancheha J V, Temperature dependence of dielectric losses in chalcogenide glasses, J. Non-Cryst. Solids., 1981, 45: 57-62

[34] Elliott S R, A theory of ac conduction in chalcogenide glasses, Philos. Mag. B., 1978, 36:291, 1978

[35] Elliott S R., Philos. Mag. B, 1978, 37, 135, doi: 10.1080/13642817808245314

How to cite this article:
Benattou H, Benramdane N, Medles M. Fabrication and investigation of structural, optical and dielectric properties of bismuth trisulfide (Bi_2S_3) thin film. J. Fundam. Appl. Sci., 2017, *9(3), 1718-1734.*